J Fluoresc (2012) 22:521–528
DOI 10.1007/s10895-011-0986-0

ORIGINAL PAPER

Optical, Structural and Thermodynamic Studies of the Association of an Anti-leucamic Drug Imatinib Mesylate with Transport Protein

Ashwini H. Hegde · Reeta Punith · J. Seetharamappa

Received: 16 July 2011 / Accepted: 16 September 2011 / Published online: 27 September 2011

Abstract The interaction of an anti-leukemic drug, imatinib mesylate (IMT) with human serum albumin (HSA) was investigated by fluorescence, synchronous fluorescence, three-dimensional fluorescence, circular dichroism and UV–vis absorption techniques under physiological condition. The process of binding of IMT on HSA was observed to be through a spontaneous molecular interaction procedure. IMT effectively quenched the intrinsic fluorescence of HSA via static quenching. The values of binding constant, number of molecules that interact simultaneously with the binding site and thermodynamic parameters were evaluated by carrying out the interactions at three different temperatures. Based on thermodynamic parameters and displacement studies with site probes, it was proposed that the drug bound at Sudlow's site I of subdomain IIA. The change in the conformation of HSA was evident from synchronous, three-dimensional fluorescence and circular dichroism studies. The distance between the donor (protein) and acceptor (drug) was calculated based on the Foster's theory of resonance energy stransfer and it was found to be 1.30 nm. The effect of different metal ions on the binding of the drug to protein was also investigated.

Keywords Human serum albumin · Spectroscopic methods · Quenching · Conformational changes

This paper was presented at 2nd DAE-BRNS symposium on atomic, molecular and optical physics organized at Department of Physics, Karnatak University Dharwad, India, from February 22 to 25, 2011.

A. H. Hegde · R. Punith · J. Seetharamappa (✉)
Department of Chemistry, Karnatak University,
Dharwad 580003, India
e-mail: jseetharam@yahoo.com

Introduction

The mesylate salt of imatinib (IMT) (Fig. 1), a tyrosine kinase inhibitor with antineoplastic activity, is designated chemically as 4-[(4-Methyl-1-piperazinyl) methyl]-N-[4-methyl-3-[[4-(3-pyridinyl)-2-pyrimidinyl] amino]-phenyl] benzamide methanesulfonate. It is used in the treatment of chronic myelogenous leukemia (CML), gastrointestinal stromal tumors (GISTs) and a number of other malignancies. Imatinib constitutes the first example of a drug that was rationally developed to block a known oncogene and which, as monotherapy, has substantially changed the biology and clinical course of a human cancer [1]. It binds to an intracellular pocket located within tyrosine kinases thereby inhibiting ATP binding by preventing phosphorylation and subsequent activation of growth receptors and their downstream signal transduction pathways. It has been shown to reduce both the smooth muscle hypertrophy and hyperplasia of the pulmonary vasculature in a variety of disease processes including portopulmonary hypertension.

Human serum albumin (HSA) is the most abundant protein constituent of blood plasma and has been used as a model protein for many and diverse biophysical and physicochemical studies [2]. He and Carter [3] have reported the three-dimensional structure of HSA through X-ray crystallographic measurements. The globular protein consists of three homologous domains that assemble to form a heart-shaped molecule, each domain contains two subdomains (A and B), and is stabilized by 17 disulfide bridges. Aromatic and heterocyclic ligands were found to bind within two hydrophobic pockets in subdomains IIA and IIIA which are consistent with site I and site II. Site I is formed as a pocket in subdomain IIA and involve the lone tryptophan of the protein (Trp-214). Site II corresponds to the pocket of subdomain IIIA, which is almost the same

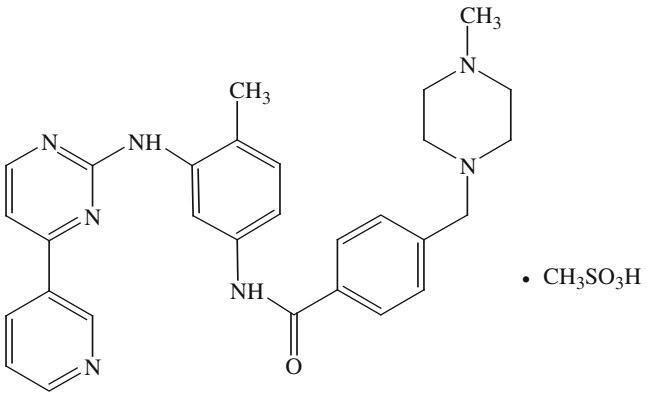

Fig. 1 Strucure of imatinib mesylate

size as site I, the interior of cavity is constituted of hydrophobic amino acid residues (Arg-410 and Tyr-411) [4, 5].

The information on the interaction of serum albumins with drugs can make us to better understand the absorption and distribution of drugs *in vivo*. In addition, the drug-albumin complex may be considered as a model for gaining general fundamental insights into the drug-protein binding. Consequently, it is important to investigate the interaction between IMT and HSA. The present study attempts to understand the mechanism of binding of IMT to protein by employing different spectroscopic techniques.

Experimental

Materials

Human serum albumin (HSA, fatty acid free) was purchased from Sigma Chemical Company, St. Louis, USA and used without further purification. Working solution of protein (250×10^{-6} mol L^{-1}) was prepared in phosphate buffer solution of pH 7.4. Pure IMT was obtained from SPR Pharma, India. A stock solution of IMT (1000×10^{-6} mol L^{-1}) was prepared in water. All other reagents and solvents were of analytical grade and doubly distilled water was used throughout the experiment. All stock solutions were stored at 4 °C.

Apparatus

Fluorescence spectra were recorded on a Hitachi spectrofluorimeter Model F-7000 (Hitachi, Japan) equipped with a 150W Xenon lamp and a slit width of 5 nm. Absorption measurements were made on a double beam CARY 50-BIO UV–vis spectrophotometer (Varian, Australia) equipped with a 150W Xenon lamp and a slit width of 5 nm. A quartz cell of 1.0 cm was used for all measurements. The CD measurements were made on a JASCO-810 spectropolarimeter (Tokyo, Japan) using a 0.1 cm cell at 0.2 nm intervals, with 3 scans averaged for each CD spectrum in the range of 200–250 nm.

Procedures

In the present investigation, the concentration of HSA was kept constant at 2.5 μM while that of the IMT was varied from 0 to 22.5 μM and from 0 to 12.5 μM for fluorescence and UV absorption studies, respectively. Fluorescence spectra were recorded at 290, 300 and 310 K in the range of 280–500 nm upon excitation at 280 nm. The absorbances of drug–protein mixtures in the concentration range employed for the experiment did not exceed 0.05 at the excitation wavelength to avoid inner filter effect.

UV absorption spectra of HSA and IMT-HSA system were noted down in the range of 200–400 nm at room temperature. The CD spectra of drug-protein mixtures (1:0, 1:1 and 1:2) were recorded in the range of 200–260 nm. The RLS spectra of HSA in the presence and absence of the drug were recorded at room temperature in the range of 250 to 650 nm with $\Delta\lambda=0$ nm. The synchronous fluorescence spectra of protein were recorded with scanning ranges, $\Delta\lambda=60$ nm and 15 nm in the absence and presence of IMT.

The three dimensional fluorescence spectra were recorded under the following conditions: the emission wavelength range 200–600 nm, the excitation wavelengths at 200–340 nm, scanning number of 15 m and increment of 10 nm with other parameters just the same as those maintained for fluorescence quenching studies.

The displacement experiments were performed using different site probes *viz*., warfarin, ibuprofen and digitoxin for site I, II and III, respectively by keeping the concentration of protein and probe, constant (2.5 μM each). The fluorescence spectra of IMT-protein system were recorded in the presence of some cations *viz*., Ca^{2+}, Ni^{2+}, Cu^{2+}, Co^{2+} and Zn^{2+} upon excitation at 280 nm. The overall concentration of HSA and common ion was maintained at 2.5 μM.

Results and Discussion

Stern-Volmer Analysis

Fluorescence quenching of protein results from the decreasing of fluorescence quantum yield. The processes such as excited state reactions, energy transfer reactions, ground-state complex formation and collisional processes resulted in quenching of protein [6]. Figure 2 shows the quenching of fluorescence intensity of HSA upon the addition of a series of amounts of IMT. Fluorescence results were

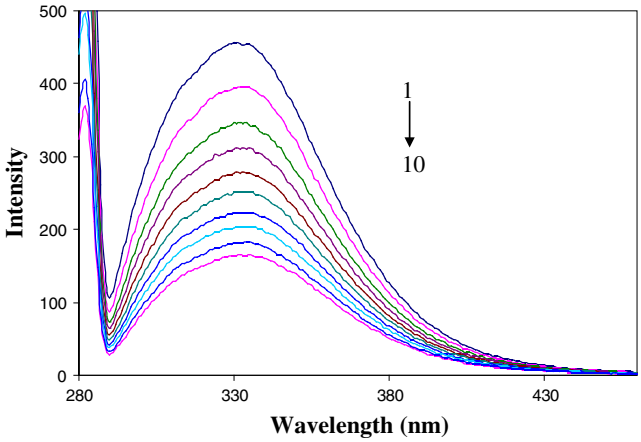

Fig. 2 Quenching of fluorescence intensity of HSA (2.5 μM) upon the addition of increasing amounts of IMT- 0 [*1*], 2.5 [*2*], 5 [*3*], 7.5 [*4*], 10 [*5*], 12.5 [*6*], 15 [*7*], 17.5 [*8*], 20 [*9*] and 22.5 μM [*10*]

subjected to Stern-Volmer analysis to understand the quenching mechanism [6]:

$$F_0/F = 1 + k_q\tau_0[Q] = 1 + K_{SV} \quad (1)$$

where F_0 and F are the fluorescence intensities of protein before and after the addition of quencher respectively, K_{SV} is the Stern–Volmer quenching constant which gives a direct measure of the quenching efficiency, k_q is bimolecular quenching rate constant, τ_0 is the average lifetime of biomolecule and [Q] is the concentration of quencher [6]. Obviously, the value of k_q can be deduced from the equation shown below:

$$K_{SV} = k_q\tau_0 \quad (2)$$

The value of τ_0 is known to be 10^{-8} s [6]. The values of K_{SV} (Table 1) are obtained from the slope of linear regression of the plots of F_0/F *versus* [Q] (Fig. 3). The k_q values were found to be in the order of 10^{12} L mol^{-1} s^{-1}. It was evident that the values of k_q were larger than the limiting diffusion constant, k_q of the biomolecule (k_q= 2.0×10^{10} L mol^{-1} s^{-1}) [7]. The decreased K_{SV} values with increase in temperature suggested that the fluorescence quenching was mainly arisen from static quenching by complex formation. Hence, the results were further analyzed by modified Stern-Volmer equation shown below [8]:

$$F_o/(F_o - F) = 1/f_aK_a[Q] + 1/f_a \quad (3)$$

where K_a is the modified Stern-Volmer association constant and f_a is the fraction of the initial fluorescence that is accessible to quencher. The plot of $F_o/(F_o$-F) *versus* 1/[Q] (Fig. not shown) yielded $f_a{}^{-1}$ as the intercept and $(f_a\ K)^{-1}$ as the slope. The value of f_a was found to be 0.738 indicating that only 73.8% of the initial fluorescence of protein was accessible for quenching. The corresponding results are shown in Table 1.

Identification of Binding Site and Thermodynamic Parameters

The values of binding constant (K) and the number of molecules that interact simultaneously with each site (n) were evaluated using the following equation [9]:

$$\log\ (F_0 - F)/F = \log K + n\ \log[Q] \quad (4)$$

The values of K and n were evaluated from the plot of log (F_0-F)/F *versus* log [Q] (Fig. not shown). The values of n close to unity indicated that one molecule of IMT interacted with single site of HSA [10].

Using the values of K, the free energy change (ΔG^0) values were calculated using the equation shown below [9]:

$$\Delta G^0 = -RT\ln K \quad (5)$$

Enthalpy change and entropy change values were calculated using the equation shown below:

$$\log K = -\Delta H^0/2.303RT + \Delta S^0/2.303R \quad (6)$$

The corresponding results are presented in Table 1. In the present study, the negative ΔG^0 values confirmed the spontaneity of interaction. From the point of view of water structure, a positive ΔS^o value was frequently regarded as evidence for hydrophobic interaction [9]. Positive ΔS^0 and negative ΔH^0 values revealed that the hydrophobic and hydrogen bonding played a major role in the interaction of IMT to protein [9].

Table 1 Binding and thermodynamic parameters of IMT-HSA interaction

T(K)	K_{SV} (L mol^{-1})	R^2	Modified Stern-Volmer constant, K_a (L mol^{-1})	*n*	ΔG^0 (KJ mol^{-1})	ΔH^0 (KJ mol^{-1})	ΔS^0 (J mol^{-1} K^{-1})
290	6.9×10^4	0.9931	1.89×10^5	1.03	−29.29		
300	6.7×10^4	0.9866	1.31×10^5	1.02	−29.39	−24.57	19.166
310	6.27×10^4	0.9926	1.03×10^5	1.04	−29.68		

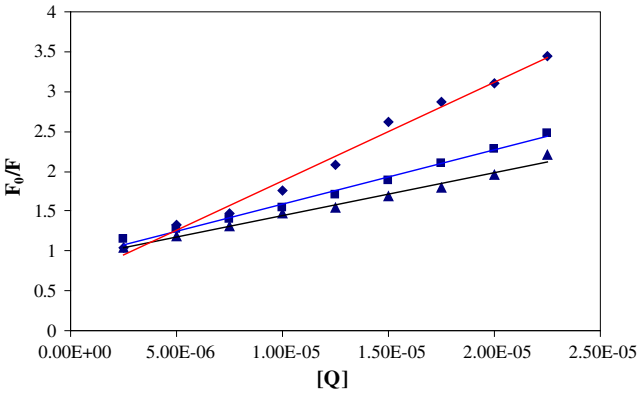

Fig. 3 The Stern-Volmer plot for binding of IMT with HSA at 290 K (*black diamond*), 300 K (*black square*) and 310 K (*black triangle*)

Site-specific Interactions of IMT at Sudlow Site I

The high-affinity binding sites on HSA have been divided into several groups according to their selectivity to the drugs. Sudlow *et al.* [11] have identified two distinct binding sites on albumin for drugs based on their abilities to displace site markers. Site I and II are commonly known as the warfarin site and diazepam site, respectively. Sudlow's site II is considered as the principal binding site for drugs. The binding site is a hydrophobic pocket and has high affinity for small aromatic ligands which may be neutral or negatively charged on periphery. Sudlow's site I consist of several adjacent and overlapping regions and can bind many diverse ligands. In the present work, the site specificity of the drug was monitored using site markers *viz.,* warfarin, ibuprofen and digitoxin for site I, II and III respectively at 300 K. The binding constant values of IMT-HSA were calculated to be 1.03×10^5, 1.34×10^5 and 1.30×10^5 M^{-1} in the presence of warfarin, ibuprofen and digitoxin, respectively. It was evident that the warfarin (site I) showed a significant displacement of IMT suggesting that both drug and warfarin compete for the same binding site on HSA. Hence, we propose that IMT bound to protein at site I subdomain IIA.

Fluorescence Resonance Energy Transfer

In order to estimate the fluorescence resonance energy transfer efficiency of the donor Trp214 and further to determine the distance of donor (HSA)–acceptor (IMT) pair, we have employed the FÖrster's theory [6]. The rate of energy transfer depends on the extent of overlapping of the emission spectrum of the donor with absorption spectrum of acceptor, the quantum yield of the donor, the relative orientation of the donor and acceptor transition dipoles, and the distance between the donor and acceptor molecules. The FÖrster distances are comparable to the size of the biomolecules and the distance between sites on multi-subunit proteins. Any condition that affects donor-acceptor distance will affect the transfer rate, allowing the change in distance to be quantified. In this type of application, one uses the extent of energy transfer between a fixed donor and acceptor to calculate the donor-acceptor distance, and thus obtain structural information about the macromolecule. For this, UV absorption spectrum of IMT was overlapped with the fluorescence emission spectrum of protein (Fig. 4). The transfer efficiency, E was measured using the average lifetime of the donor in the absence (F_0) and presence of acceptor (F) as follows [12]:

$$E = 1 - F/F_o = R_o{}^6/\left(R_o{}^6 + r^6\right) \tag{7}$$

where R_o is the critical distance when the transfer efficiency is 50% and it is given by the equation [13]:

$$R_o{}^6 = 8.8 \times 10^{-25}\kappa^2\eta^{-4}\Phi J \tag{8}$$

where κ^2 is a factor describing the relative orientation in space of the emission and absorption transition dipoles of the donor and acceptor, respectively. J is the overlap integral which expresses the degree of spectral overlap between the donor emission and the acceptor absorption. The value of J is obtained using the equation below [14]:

$$J = \Sigma F(\lambda)\varepsilon(\lambda)\lambda^4\Delta\lambda/\Sigma F(\lambda)\Delta\lambda \tag{9}$$

where $F(\lambda)$ is the fluorescence intensity of the donor and $\varepsilon(\lambda)$ is the extinction coefficient of the acceptor at λ, $\kappa^2=2/3$, $\eta=1.336$ and $\Phi=0.118$ [15]. From Eqs. (7) to (9), we obtained that $J=0.829\times10^{-14}$ cm^3 L mol^{-1}, $E=0.5807$, $R_0=2.54$ and $r=1.30$ nm.

The calculated binding distance (r) was lower than 8 nm, and fulfilled the condition, $0.5R_0<r<1.5R_0$ [16] which indicated that the non-radiation energy transfer occurred from HSA to IMT.

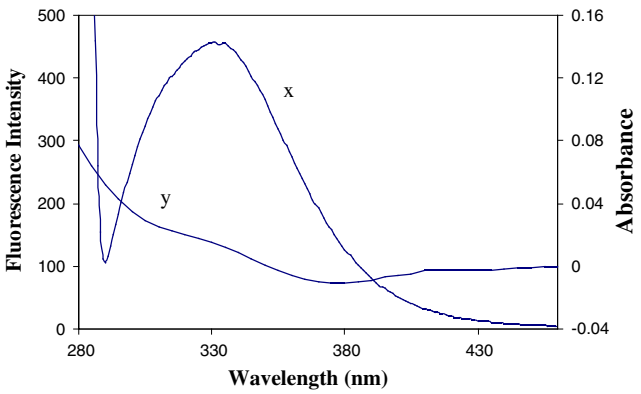

Fig. 4 The overlap of fluorescence spectrum of HSA [x] with absorption spectrum of IMT [y]

The Effect of Metal Ions on Binding

Some plasma proteins (serum albumin) usually act as elimination agent of metal ions and have a variety of metal sites with different specificities. This phenomenon of serum albumin molecular conformational alteration caused by metal ions-HSA binding could be observed in some metal ions-HSA interaction process. Furthermore, many metal ions could form complexes with medicinal molecules, and affect some properties of drug. They would affect the interaction of medicinal molecule-HSA in a ternary system of drug-protein-metal ion, and thus it would influence the distribution, pharmacological property, and metabolism of medicine in blood. In view of this, the binding aspect of IMT-HSA was investigated in the presence of common ions *viz*., K^+, Co^{2+}, Cu^{2+}, Ni^{2+} and Mn^{2+} at 300 K. As evident from Table 2, the binding constant values of IMT-HSA decreased in the presence of the above ions indicating the shortening of storage time of drug in blood plasma. All these results indicated that the quenching efficiency of drug was influenced by the metal ions.

Characteristics of RLS Spectra

Resonance light scattering spectroscopy (RLS) is a sensitive and selective technique for monitoring molecular assemblies which can provide some insights into the interaction [14]. RLS is an elastic scattering that occurs when an incident beam is close to an absorption band. Pasternack et al. established this technique to study biological macromolecules employing an ordinary fluorescence spectrometer [17].

The RLS spectra of HSA, IMT and HSA–IMT complex were recorded by synchronously scanning from 240 to 600 nm with $\Delta\lambda$=0 nm. The results are shown in Fig. 5. Upon the addition of trace amounts of IMT to HSA solution, a remarkably increased RLS was observed. The production of RLS was correlated with the formation of certain aggregate [18] and the RLS intensity was dominated primarily by the particle dimension of the formed aggregate in solution. So, it was proposed that the enhanced RLS intensity observed in the present study was due to the formation of HSA–IMT complex.

Table 2 Effects of common ions on binding of IMT to HSA

System	Association constant (M^{-1})
HSA+IMT	1.31×10^5
HSA+IMT+K^+	1.18×10^5
HSA+IMT+Co^{2+}	1.11×10^5
HSA+IMT+Cu^{2+}	1.07×10^5
HSA+IMT+Ni^{2+}	1.23×10^5
HSA+IMT+Mn^{2+}	1.26×10^5

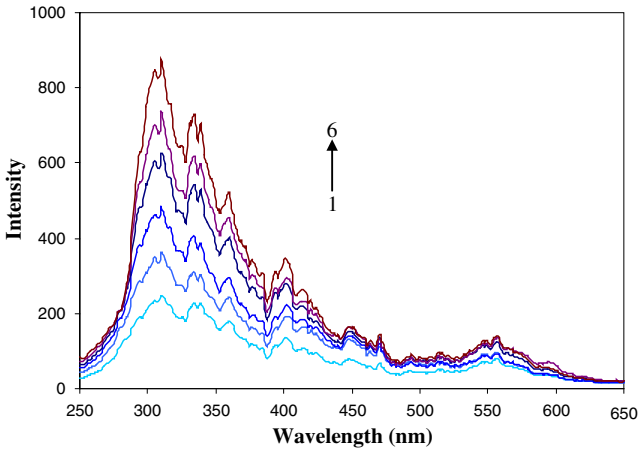

Fig. 5 Resonance light scattering spectra of HSA (2.5 μM) with increasing concentrations of IMT- *1*) 0, *2*) 2.5, *3*) 5, *4*) 7.5, *5*) 10, *6*) 12.5 μM

Investigation of Conformational Changes

Absorbance Measurements

The UV absorption spectrum of IMT showed a broad band with absorption maximum at around 255 nm while HSA has a strong absorption band at 280 nm (Fig. 6). With gradual addition of IMT, the absorbance of HSA gradually increased. This enhancement of absorption of HSA in the presence of IMT appeared to be initially due to the formation of a complex from the intermolecular interactions and further results exhibited a concentration dependent relationship. In addition, the λ_{max} of HSA showed a slight

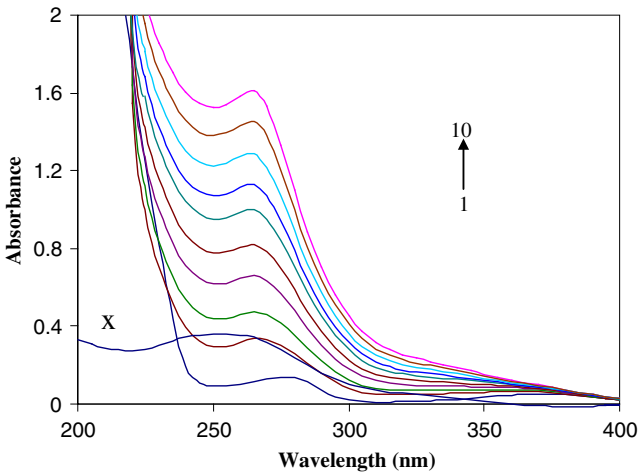

Fig. 6 Absorption spectra of HSA and IMT-HSA system. HSA concentration was maintained at 2.5 μM [*1*] and that of IMT was varied- 2.5 [*2*], 5 [*3*], 7.5 [*4*], 10 [*5*], and 12.5 μM [*6*]. [x] is the absorption spectrum of only IMT (2.5 μM)

blue shift of 15 nm (from 280 to 265 nm). These results indicated that the interaction between IMT and HSA altered the microenvironment around HSA.

Synchronous Fluorescence

Synchronous fluorescence is a useful tool to investigate the microenvironment around the fluorophore groups. As is known, synchronous fluorescence spectra represent tyrosine residues of HSA only at the wavelength interval ($\Delta\lambda$) of 15 nm and tryptophan residues only at $\Delta\lambda$ of 60 nm [19]. The synchronous fluorescence spectra of HSA in the absence and presence of increasing amounts of IMT were scanned at $\Delta\lambda$=60 nm and 15 nm. The fluorescence of tryptophan (Fig. 7) decreased with the addition of increasing amounts of IMT and the λ_{max} was found to be shifted from 341 to 349 nm. However, the fluorescence intensity of tyrosine was noticed to be weak (Fig. not shown). Further, no shift in maximum emission wavelength (λ_{max}) was noticed upon the addition of IMT. The red shift in λ_{max} of tryptophan emission suggested that the polarity around tryptophan increased where as the hydrophobicity of protein decreased. This indicated that the interaction between IMT and HSA significantly affected the conformation of tryptophan residue micro region.

Circular Dichroism

The albumin structure is predominantly α-helical. Approximately, 67% of HSA is helical, the remaining secondary structure consists of 10% β-turns and 23% extended peptide chain. The CD spectra of the HSA exhibited two negative bands in the ultraviolet region at 209 and 222 nm characteristic of α -helical structure of the protein. Upon the addition of IMT to HSA, the α-helicity of protein decreased and hence, the reduced intensity of double minimum was observed (Fig. 8). The CD results are expressed in terms of mean residue ellipticity (MRE) in deg cm^2 $dmol^{-1}$ according to the equation shown below:

$$\text{MRE} = \text{observed CD (mdeg)}/\left[C_p nl \times 10\right] \quad (10)$$

where C_p is the molar concentration of protein, n is the number of amino acid residues and l is the path length. The α-helical contents of free and combined HSA are calculated from MRE values at 208 nm using the equation given below [20]:

$$\alpha - \text{helix}(\%) = [(-\text{MRE}_{208} - 4000)/(33000 - 4000)] \times 100 \quad (11)$$

where MRE_{208} is the observed MRE value at 208 nm, 4000 is the MRE of the α-form and random coil conformation cross at 208 nm and 33,000 is the MRE value of a pure α-helix at 208 nm. Using the above equation, the α-helicity in the secondary structure of HSA was determined. It decreased from 66.58% in free HSA to 58.49% in IMT-HSA. The CD spectra of HSA were observed to be similar in shape in the presence and absence of IMT indicating that the structure of HSA was also predominantly α-helical [21]. Therefore, we propose that the binding of IMT to HSA induced changes in secondary structure of HSA.

Three Dimensional Fluorescence

Three-dimensional fluorescence contour map is a rising fluorescence analysis technique in recent years. The excitation wavelength, the emission wavelength and the fluorescence intensity can be used as axes to investigate the integrated information of the samples, and the contour spectra provide a lot of important information [22]. Figure 9 represented the projection spectra and contour map of HSA (9a and 9c) and IMT–HSA (9b and 9d), respectively. In Fig. 9c, peak 1 and peak 2 are the Raleigh scattering peaks

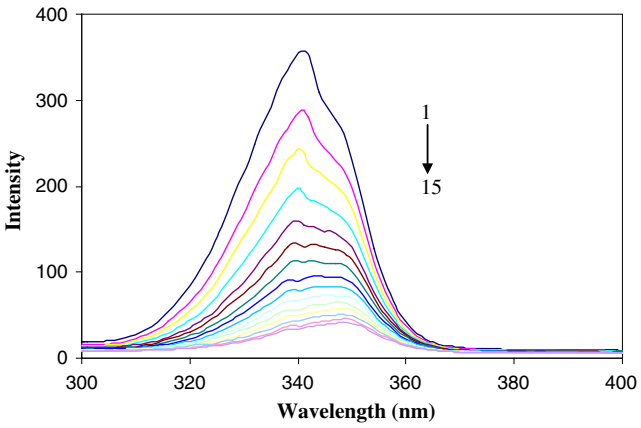

Fig. 7 The effect of IMT on synchronous fluorescence spectra of HSA- (**a**) $\Delta\lambda$=15 nm; (**b**) $\Delta\lambda$=60 nm. [HSA]=2.5 μM [*1*]; [IMT]= 2.5 [*2*], 5 [*3*], 7.5 [*4*], 10 [*5*], 12.5 [*6*], 15 [*7*], 17.5 [*8*], 20 [*9*], 22.5 [*10*], 25 [*11*], 27.5 [*12*], 30 [*13*], 32.5 [*14*] and 35 μM [*15*]

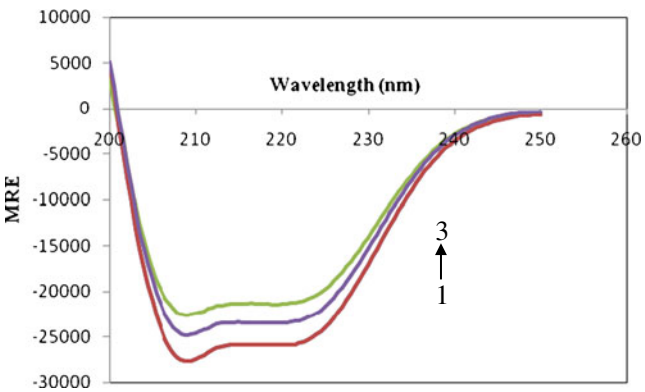

Fig. 8 CD spectra of HSA (5 μM) in the absence [*1*] and presence of 5 [*2*] and 10 μM [*3*] of IMT

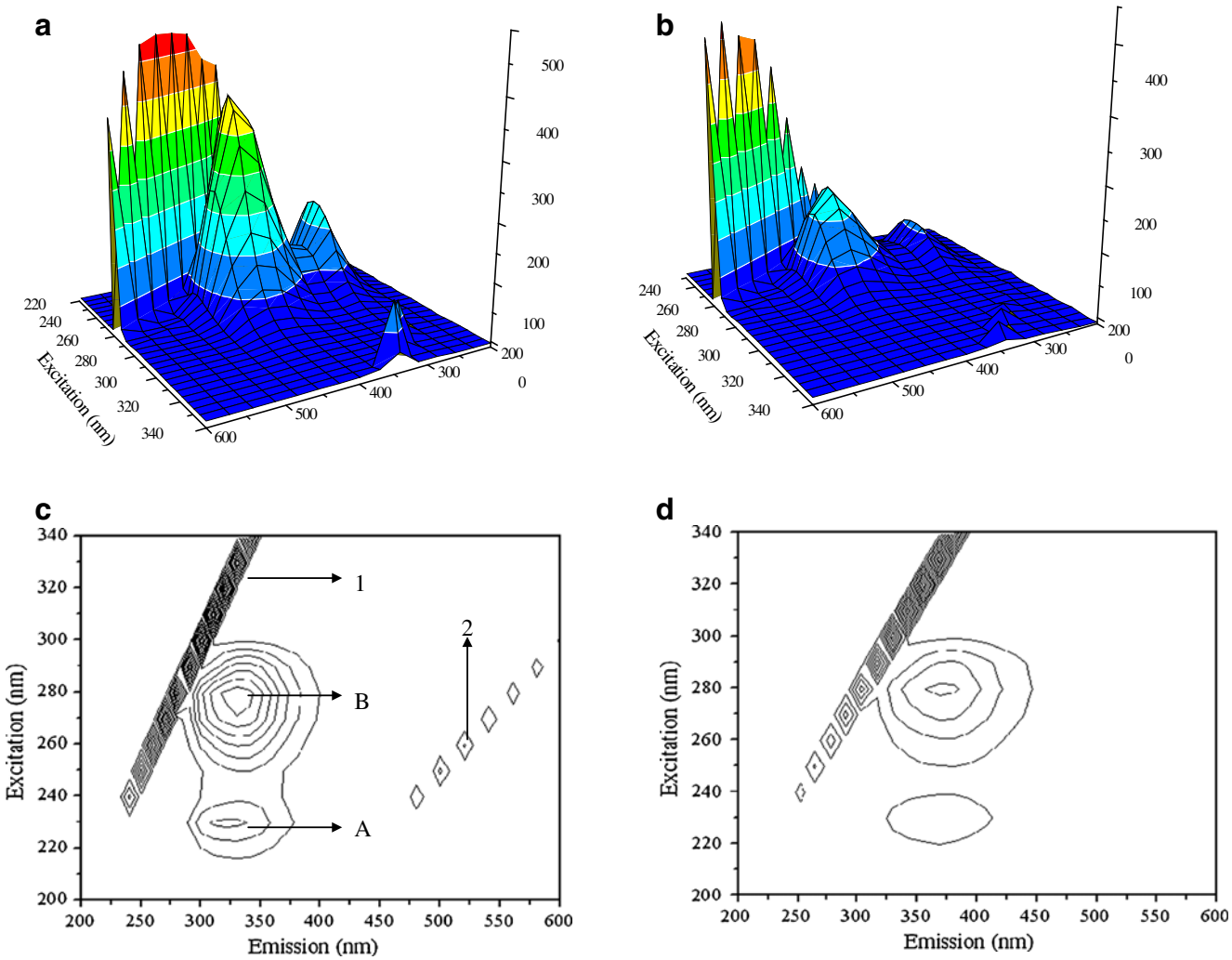

Fig. 9 The three-dimensional fluorescence spectra and corresponding contour diagrams of HSA (**a** and **c**) and IMT–HSA (**b** and **d**). [HSA]= 2.5 μM and [IMT]=22.5 μM

($\lambda_{ex}=\lambda_{em}$) and the second-ordered scattering peaks ($\lambda_{em}=2\lambda_{ex}$). Two typical fluorescence peaks (peak A: $\lambda_{ex}/\lambda_{em}$= 230/320 nm; peak B: $\lambda_{ex}/\lambda_{em}$=280/330 nm) could be easily observed in three-dimensional fluorescence contour map of HSA. The excitation wavelength of peak A observed at 230 nm provided some clues to investigate the characteristics of this peak due to n → π* transition of HSA's characteristic polypeptide backbone structure, C = O. Besides peak A, there was another new strong fluorescence peak B that revealed the intrinsic fluorescence of tryptophan and tyrosine residues. The intensity of peak A and peak B was found to be decreased to different degrees (Table 3). This phenomenon showed that the binding of IMT induced some micro-environmental and conformational changes in HSA.

Conclusions

The present paper describes the interaction of an antileucamic drug with HSA as investigated by absorption, fluorescence, RLS and CD techniques for the first time.

Table 3 Three-dimensional fluorescence spectral parameters for HSA in the absence and presence of IMT

System	Peak 1 (nm)		Δλ (nm)	Intensity	Peak 2 (nm)		Δλ (nm)	Intensity
	λ_{ex}	λ_{em}			λ_{ex}	λ_{em}		
HSA	230	320	90	153.6	280	330	50	45.55
HSA-IMT	230	320	90	371.0	280	330	50	123.2

As evident from absorption and RLS studies, there was a formation of ground state complex between IMT and protein. Further, the synchronous and 3D fluorescence measurements revealed the microenvironmental changes around tryptophan moiety of the protein upon binding with IMT. CD studies also indicated the changes in secondary structure of the protein upon binding to IMT.

Acknowledgements We are grateful to the Council of Scientific and Industrial Research, New Delhi, for financial assistance (grant No. 01 (2279)/08/EMR-II dated 20-11-2008). The author (A.H. Hegde) thanks the UGC, New Delhi for the award of meritorious Fellowships in Science. Thanks are also due to the authorities of the Karnatak University, Dharwad, for providing the necessary facilities.

References

1. Gambacorti-Passerini C (2008) Part I: Milestones in personalised medicine–imatinib. Lancet Oncol 9:600
2. Abou-Zied OK, Al-Shihi OI (2008) Characterization of subdomain IIA binding site of human serum albumin in its native, unfolded, and refolded states using small molecular probes. J Am Chem Soc 130:10793–801
3. Carter DC, Ho JX (1994) Structure of serum albumin. Adv Protein Chem 45:153–203
4. Sugio S, Kashima A, Mochizuki S, Noda M, Kobayashi K (1999) Crystal structure of human serum albumin. Prot Eng Design Select 12:439–446
5. Kragh-Hansen U, Chuang VTG, Otagiri M (2002) Practical aspects of the ligand binding and enzymatic properties of human serum albumin. Biol Pharm Bull 25:695–704
6. Lakowicz JR (2006) Principles of fluorescence spectroscopy. Springer Publications, New York, p 11, 445
7. Vaughan WM, Weber G (1970) Oxygen quenching of pyrenebutyric acid fluorescence in water: a dynamic probe of the microenvironment. Biochemistry 9:464–473
8. Lehrer SS (1971) Solute peturbation of protein fluorescence. The quenching of the tryptophyl fluorescence of model compounds and of lysozyme by iodide ion. Biochemistry 10:3254–3263
9. Ross PD, Subramanian S (1981) Thermodynamics of protein association reactions: forces contributing to stability. Biochemistry 20:3096–3102
10. Lissi E, Abuin E (2011) On the evaluation of the number of binding sites in proteins from steady state fluorescence measurements. J Fluoresc 21:1831–1833
11. Sudlow G, Birkett DJ, Wade DN (1975) The characterization of two specific drug binding sites on human serum albumin. Mol Pharmacol 11:824–832
12. Horrocks WD, Collier WE (1981) Lanthanide ion luminescence probes. Measurement of distance between intrinsic protein fluorophores and bound metal ions: quantitation of energy transfer between tryptophan and terbium(III) or europium(III) in the calcium-binding protein parvalbumin. J Am Chem Soc 103:2856–2862
13. Sklar LA, Hudson BS, Simoni RD (1977) Conjugated polyene fatty acids as fluorescent probes: synthetic phospholipid membrane studies. Biochemistry 16:819–828
14. Ge F, Jiang L, Liu D, Chen C (2011) Interaction between alizarin and human serum albumin by fluorescence spectroscopy. Anal Sci 27:79–84
15. Trnkova L, Boušova I, Staňkova V, Dršata J (2011) Study on the interaction of catechins with human serum albumin using spectroscopic and electrophoretic techniques. J Mol Struct 985:243–250
16. Shi XY, Cao H, Ren FL, Xu M (2007) Spectroscopic analysis of the binding interaction between tinidazole and bovine serum albumin. Chem Biodiver 4:2780–2790
17. Pasternack RF, Bustamante C, Colling PJ, Giannetto A, Gibbs EJ (1993) Porphyrin assemblies on DNA as studied by a resonance light scattering technique. J Amer Chem Soc 115:5393–5399
18. Anglister J, Steinberg IZ (1983) Resonance Rayleigh scattering of cyanine dyes in solution. J Chem Phys 78:5358–5368
19. Miller JN (1979) Recent advances in molecular luminescence analysis. Proc Anal Div Chem Soc 16:203–208
20. Lu ZX, Cui T, Shi QL (1987) Applications of circular dichroism and optical rotatory dispersion in molecular biology, 1st edn. Science Press, pp 79–82
21. Ding F, Liu W, Li N, Zhang L, Sun Y (2010) Complex of nicosulfuron with human serum albumin: a biophysical study. J Mol Struct 975:256–264
22. Wang YQ, Zhang HM, Wang RH (2008) Investigation of the interaction between colloidal TiO_2 and bovine hemoglobin using spectral methods. Colloids and Surfaces B: Biointerfaces 65:190–196